

A criterion for the generation of turbulent anabatic flows

M. Princevac^{a)}

Department of Mechanical Engineering, University of California at Riverside, Riverside, California 92521, USA

H. J. S. Fernando

Department of Mechanical and Aerospace Engineering, Arizona State University, Tempe, Arizona 85287, USA

(Received 30 January 2007; accepted 26 July 2007; published online 3 October 2007)

Turbulent convection over a heated infinite horizontal plane is ideally characterized by updrafts and downdrafts with no net mean motion, but a mean upslope (or anabatic) flow can be generated if the plane is even slightly inclined. A study on the mechanism responsible for the generation of upslope flow is described in this paper. When the heat flux is sufficiently large, the upslope flow becomes turbulent and is signified by thermals rising from the surface and deflected upslope to feed into the anabatic flow. It is argued theoretically and demonstrated experimentally that for a certain Prandtl number (Pr) range the tendency for heated thermals to deflect and follow the slope is inversely proportional to Pr and directly proportional to the inclination angle (β), and thus the critical angle above which the upslope flow can be sustained is given by $\beta_c = c Pr$, where c is a constant. This finding can explain the existence of well-developed atmospheric ($Pr \sim 1$) upslope flows above very gentle slopes in areas of complex topography. © 2007 American Institute of Physics.

[DOI: [10.1063/1.2775932](https://doi.org/10.1063/1.2775932)]

I. INTRODUCTION

The world's population centers are often located in topography replete with mountains, valleys, escarpments, and basins, commonly known as complex terrain. In the absence of large-scale weather systems, flow in these areas is dominated by diurnal variation of local solar heating, i.e., cooling at night and heating during the day, which leads to two wind systems: slope and valley winds, as indicated in Fig. 1. The formation mechanisms and dynamics of downslope (katabatic) and down-valley winds occurring at night have been well studied using laboratory and numerical modeling as well as field studies,¹⁻³ but the corresponding work on daytime upslope (anabatic) and up-valley flows is lesser, perhaps because their profound role in air pollution dispersion has not been fully realized until recently. While nocturnal stable flows trap pollutants close to the ground (\sim tens of meters) and disperse horizontally via meandering motions, daytime upslope convective flows mix pollutants over a greater height (\sim 1 km) and transport them over longer distances. The latter mode of pollution distribution is crucial, given that typical cities are located in plains surrounded by sloping terrain and that upslope flows carry pollutants from urban/city areas to suburban (elevated) mountain slopes with high-end residential real estate.^{4,5} Field studies have shown that upslope flows can effectively transport pollutants and their precursors tens of kilometers within a day, causing pristine suburban areas to bear the brunt of urban pollution.⁴⁻⁶ Certain pollutant precursors, while being transported by upslope flow, collude with turbulent mixing and intense sunlight to generate additional hazardous pollutants such as ozone.⁶ As

such, upslope flows are at the heart of contemporary urban air pollution studies.

This paper deals with the generation of upslope flows, in particular, the critical angle that is necessary to generate an upslope flow in contrast to the genesis of classical up- and downdraft dominated convection intrinsic to flat terrain. This work complements our previous theoretical work on fully developed upslope flows⁷ as well as a suite of observational and numerical studies reported on upslope and up-valley flows.⁸⁻¹³ A major contribution to the theoretical analysis of the steady problem was made by Prandtl¹⁴ who derived profiles of wind and temperature for a given two-dimensional uniform slope with a fixed surface temperature. Egger¹⁵ extended this analysis to the case of varying surface temperature along the slope. Although the simplified analysis of Prandtl has been applied to real atmospheric situations with the assumption of constant "eddy" coefficients, numerous works^{7,16} suggest that this assumption is unjustifiable. Other modeling approaches, including large eddy simulations (LES) (Refs. 16 and 17) and phenomenological modeling have been used with atmospheric applications in mind. For example, Vergeiner and Dreiseitl¹⁸ considered the energy balance in a valley and associated slope flow to derive an expression for the upslope volumetric flow rate. Hunt *et al.*⁷ presented a theoretical analysis on the mean upslope velocity and flow structure. Only a handful of laboratory experiments have been reported on upslope flows.¹⁹⁻²¹

To explain the generation of up-valley flows, Whiteman^{1,2} considered the simple topographic configuration of a valley adjacent to a plain (e.g., Fig. 1). He argued that the daytime temperature of the valley should be higher than that of the contiguous plane because of the low air volume containing in the former (for a given solar insolation),

^{a)}Telephone: 951-827-2445. Fax: 951-827-2899. Electronic mail: marko@engr.ucr.edu

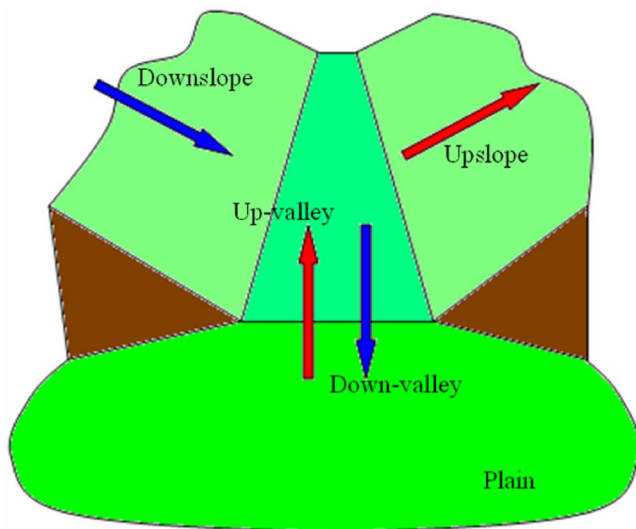


FIG. 1. (Color online) A schematic of slope and valley wind systems.

which causes a hydrostatic pressure differential to build up and drive the up-valley flow. Rampanelli *et al.*²² demonstrated that upslope flow along the valley walls can amplify this pressure difference, thus pointing to the importance of the interaction between slope and valley flows. Although general dynamical aspects of upslope flow phenomena have been well studied^{2,7,19,23} and it is known that plumes above sloping boundaries bend along-slope rather than rising vertically,²⁴ no explicit theoretical formulation is available to describe the genesis of upslope flows nor have there been a reported criterion to ascertain whether heating of a given slope can produce an upslope flow.

As an antecedent to the development of a theoretical model, herein we propose a mechanism for the formation of slope flows on an inclined plane subjected to surface heating. As argued by Howard²⁵ and demonstrated in laboratory experiments,^{26,27} high Rayleigh number (Ra) turbulent thermal convection on a horizontal plane is initiated via thermals (heated blobs) rising vertically due to sporadic breakdown of the thermal boundary layer; see Fig. 2(a) (all photographs

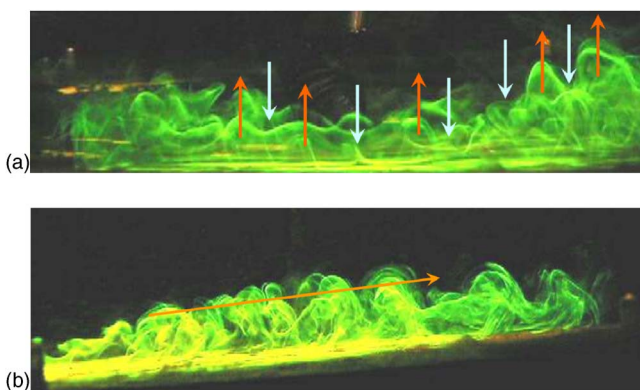


FIG. 2. (Color online) (a) Experimental visualization of convection above a horizontal heated plate. Updraft and downdraft regions are marked. There is no mean flow along the plate. (b) Experimental visualization of convection above the sloped heated plate. Thermal blobs are sliding along the plate forming the mean upslope motion.

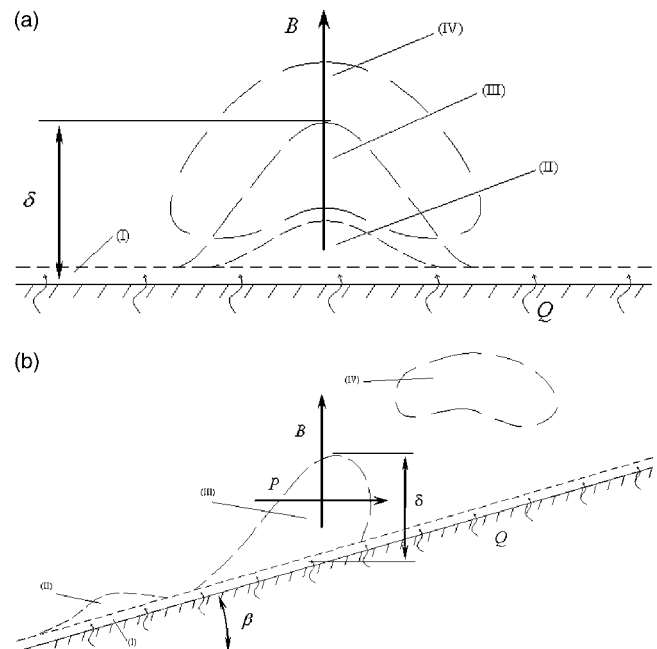


FIG. 3. (a) Development of the thermal blob on the uniformly heated horizontal plate: (I) initial thermal boundary layer; (II) instability (thermal blob) appears and starts to grow; (III) fully formed thermal blob; (IV) after reaching critical size blob detaches and starts vertical rise. Presented on the schematic are surface heat flux Q , buoyancy force B , and the blob size δ . (b) Development of thermal blob on a uniformly heated inclined plate: (I) initial thermal boundary layer grows and slides upslope; (II) instability (thermal blob) appears, starts to grow and continues sliding upslope; (III) thermal blob keeps on growing and sliding; (IV) after reaching a critical size and traveling a certain upslope distance the blob detaches and starts its free rise. Presented on the schematic are surface heat flux Q , buoyancy force B , pressure force P , slope angle β , and the blob size δ .

were taken from our experiments, see Secs. III and IV). When the plane is inclined, however, a horizontal pressure gradient can be developed across rising thermals, causing them to cling on to the surface (Coanda effect²⁸), thus deflecting the thermals upslope [Fig. 2(b)]. By considering two competing tendencies, one responsible for the vertical rise of thermals and the other favoring along-slope sliding, a phenomenological criterion is advanced in Sec. II to predict the conditions under which upslope (anabatic) flow prevails over rising thermals. The main interest is on high heat-flux (or turbulent convection) conditions with possible applications to atmospheric convection in complex terrain. The flow configuration in point is simple, in that the fluid is neutrally stratified (homogeneous), the slope is constant and smooth and the heat flux is stationary and spatially uniform. Laboratory experiments to verify theoretical predictions are described in Sec. III. The results of the experiments are given in Sec. IV, followed by a summary in Sec. V.

II. THEORETICAL ANALYSIS

As the base case, consider turbulent convection over a horizontal heated plate, as shown in Fig. 3(a). According to the classical model proposed by Howard,²⁵ turbulent convection on a flat surface is maintained by the development and breakdown of a molecular boundary layer near the surface. The thickness δ of this boundary layer grows with time t

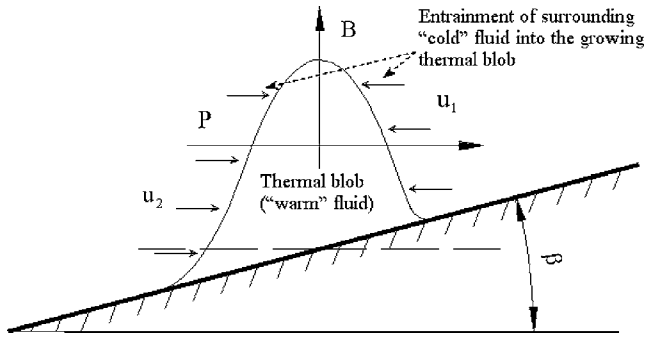


FIG. 4. A schematic of the thermal blob at the detachment from the inclined surface. Note the vertical buoyancy force, B , and horizontal pressure gradient force, P , which is a consequence of the asymmetric fluid entrainment into the blob. The entrainment velocities from the down-facing (u_2) and the up-facing (u_1) sides of the blob are also illustrated.

according to $\delta \sim c_1(\kappa t)^{1/2}$, where c_1 is a constant of the order one and κ the thermal diffusivity, and then breaks down to form rising thermals [heated mushroom-like fluid blobs; Figs. 2(a) and 3(a)] after reaching a critical Rayleigh number

$$\text{Ra}_c = \frac{g\alpha\Delta T\delta_c^3}{\nu\kappa} \approx 10^3, \quad (1)$$

where g is the gravitational acceleration, α is the thermal expansion coefficient, δ_c is the limiting value of δ at the breakdown, ΔT is the temperature difference between the thermal and (reference) background fluid of density ρ_0 , and ν is the kinematic viscosity. The density of the fluid is expressed using the equation of state $\rho = \rho_0(1 - \alpha\Delta T)$. Upon removal of boundary-layer fluid via rising (detached) thermals, a new boundary layer is formed, and the sequence of growth/breakdown events continues, intermittently releasing buoyant thermals that feed into convection.

Conversely, for the case of an incline, there are two major driving forces: buoyancy force that drives the flow vertically upward and horizontal pressure gradient that causes flow to cling on to the inclined surface and slide along it [Fig. 3(b)]. The ratio of these forces is expected to determine whether the thermals detaching from the boundary layer rise vertically [Figs. 2(a) and 3(a)] or slide along the incline to support upslope flow [Figs. 2(b) and 3(b)]. Experiments [see Sec. IV and Figs. 2(b), 7, and 9] show that in the latter case the thermals travel along the slope for some distance and then detach to feed into the turbulent anabatic layer. Note that the molecular diffusive thermal boundary layer just above the incline is different in character from the overlying turbulent boundary layer, and thermals from the former help drive the latter. For the case of typical fully developed turbulent convection in the atmosphere, the role of these thin molecular boundary layers is insignificant given that roughness lengths outweigh the molecular layers. At the onset of convection, however, molecular-diffusive layers may still play a role.

A schematic of buoyancy B and pressure gradient ($-\partial p/\partial x$) forces acting on a turbulent thermal on an incline is shown in Fig. 4. Initial motion inside the thermal boundary layer [Fig. 3(b)] is determined by a balance between viscous and buoyancy forces,

$$\bar{U}_b \frac{\bar{U}_b}{\delta^2} \sim \alpha g \Delta T \beta, \quad (2)$$

where \bar{U}_b is the averaged along-slope flow velocity and β is the slope angle (which is considered to be small such that $\sin \beta \approx \beta$). Note that the symbol \sim is used to denote the order of magnitude estimate. In Eq. (2), it is assumed that the momentum and thermal boundary layers are on the same order (δ), and thus $\text{Pr}^{1/2} \sim 1$. The heat balance in the boundary layer takes the form

$$Qt \approx c_p \rho_0 \Delta T \delta, \quad (3a)$$

where t is the time, Q is the bottom heat flux, and c_p is the specific heat. This energy balance can be expressed via buoyancy flux as

$$q_0 t \approx g \alpha \Delta T \delta, \quad (3b)$$

where q_0 is the buoyancy flux at the bottom boundary, $q_0 = \alpha g Q / \rho_0 c_p$. From Eqs. (2) and (3b), \bar{U}_b can be expressed as

$$\bar{U}_b \sim \beta \frac{q_0 t \delta}{\nu}. \quad (4)$$

The time scale over which the blob will travel along the slope before it separates thus can be estimated from Eqs. (1) and (3b) as

$$t_c \approx c_1^{-1} \left(\frac{\text{Ra}_c \nu}{q_0} \right)^{1/2}, \quad (5)$$

where in the initial stages of flow development the thermal layer depth grows according to $\delta \approx c_1(\kappa t)^{1/2}$. The length of travel before the detachment occurs can be estimated as

$$L \sim \int_0^{t_c} \bar{U}_b dt \sim \frac{2}{5} c_1^{-3/2} \beta \frac{\text{Ra}_c^{5/4}}{\text{Pr}^{1/2}} \left(\frac{\nu^3}{q_0} \right)^{1/4}, \quad (6)$$

which is on the order of several centimeters. These motions set the wall conditions for the upslope flows, and thermals emanating from this upward sliding molecular-diffusive layer deflect and provide forcing for the upslope turbulent flow. The rising thermals are expected to be deflected towards the slope by horizontal pressure gradients arising from asymmetric entrainment of background fluid into them.

The buoyancy force B associated with the thermal can be estimated as

$$B \sim (\rho_0 - \rho) g \delta^3 = \rho_0 \alpha g \Delta T \delta^3, \quad (7)$$

where the size of the blob is taken as the boundary layer thickness.²⁹ Assuming the same entrainment flow rate into the blob from the up and downslope facing sides, the pressure force P can be written as

$$P \sim \Delta p \delta^2 \sim \rho_0 (u_1^2 - u_2^2) \delta^2, \quad (8)$$

where u_1 and u_2 are the entrainment velocities from the sides of the thermal as shown in Fig. 4 and Δp is the pressure differential across the blob. The pressure gradient can be estimated based on the above assumption that detaching thermals entrain the same total volume of fluid from all directions, and hence the characteristic entrainment velocity of the

downslope facing side of the thermal (u_2) is lower than the upslope facing side (u_1), viz.,

$$U\delta^2 \sim u_1\delta^2(1 - \beta) = u_2\delta^2(1 + \beta), \quad (9)$$

where U is the characteristic velocity of the entrainment flow based on total entrainment due to rising thermal. The horizontal pressure differential, thus, can be scaled as

$$\Delta p \sim \rho_0 U^2 \beta, \quad (10)$$

which gives

$$P \sim \Delta p \delta^2 \sim \rho_0 U^2 \beta \delta^2. \quad (11)$$

The characteristic velocity of the entrainment flow into the thermal at the detachment can be scaled as $U \sim \delta_c / t_c$. Using Eqs. (3a), (1), and (5), δ_c can be expressed as $\delta_c \approx (c_1^2 \text{Ra}_c)^{1/4} (\kappa^2 \nu / q_0)^{1/4}$ and U as $U \sim (c_1^6 / \text{Ra}_c)^{1/4} (\kappa^2 q_0 / \nu)^{1/4}$. Using Eqs. (1) and (7), the buoyancy force can be expressed as

$$B \sim \rho_0 \text{Ra}_c \kappa \nu, \quad (12)$$

and similarly from Eqs. (11) and (5) the pressure force can be expressed as

$$P \sim c_1^4 \rho_0 \beta \kappa^2. \quad (13)$$

The ratio of these two forces in vertical and horizontal directions, respectively, can be written as

$$\frac{B}{P} \sim \left(\frac{\text{Ra}_c}{c_1^4} \right) \frac{\text{Pr}}{\beta}. \quad (14)$$

The ratio B/P is expected to determine whether the detaching thermals rise vertically or cling on and flow along the slope. The upslope flow is possible, say, for $B/P < \gamma$, where γ is a critical value, and thus the critical angle above which a sustained upslope flow is possible is given by $\beta_c = c \text{Pr}$. Here c is a constant that is comprised of all proportionality constants used; given the exponents and the nature of the proportionality constants involved, it is not expected to be of order unity. Note that this formulation is only valid for sufficiently high heat fluxes where the flow breaks down into sustained turbulence from the very inception (i.e., appropriate Rayleigh numbers are much higher than that is required for linear stability). A laboratory experiment designed to verify this formulation is described below.

III. EXPERIMENTAL SETUP

The experiments were carried out in a tank with a cross section of 60×60 cm and a depth 70 cm, constructed with Plexiglas sidewalls (1.25 cm thick) and an aluminum bottom (1 cm thick); see Fig. 5. The heating system lay beneath the aluminum plate and consisted of a custom designed heating pad insulated from below by two layers of 1.25 cm marsornite sheet, a single layer of 2.5 cm thick foam insulation, and a 0.8 cm thick aluminum base plate. Insulation from the sides was provided by 2.5 cm foam sheets. A removable window in the sidewall insulation allowed optical access to visualize the flow. The heating pad was custom designed by Watlow, Inc. and consisted of an array of closely spaced heating wires embedded in a conducting seating (base) ma-

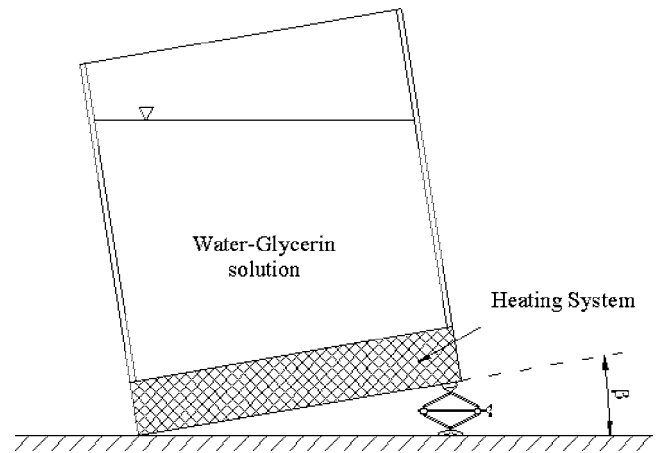


FIG. 5. A schematic of the experimental apparatus.

terial, the maximum total heat output being 1 kW/m^2 . The heat flux was regulated using a rheostat. The slope angle of the bottom heating plate was realized by uniformly elevating one side of the tank using a precision adjustable jack. The beam of a small laser diode attached to a tank wall, parallel to the slope, was projected on to a screen placed 2 m from the tank, and the position of its image was used to measure the inclination of the heating plate. The resolution of inclination measurements was 0.125° . In the experimental planning, the apparatus was tested to ensure uniformity of temperature distribution along the slope. It is noteworthy that an apparatus designed with a longer slope length of 2 m and heating provided by a heat exchanger had to be abandoned due to failure of realizing temperature uniformity along the slope. The rheostat was calibrated by measuring the temperature rise of a 15 cm layer of water in the tank over a time period of 30 min, in the absence of the slope. Here the heat input was calculated considering the energy balance of the water layer and losses (which were estimated using the technique used by Voropayev and Fernando,³⁰ to be less than $\pm 4\%$). These measurements agreed within $\pm 6\%$ with independent flux measurements made using a heat flux meter.

A glycerin and water mixture was used as the working fluid, allowing a wide range of Prandtl numbers by changing the mixture composition. The typical averaged fluid depth was ~ 50 cm. The dependence of Prandtl number of the glycerin-water solution on temperature was determined using the regression analysis results given by Shankar and Kumar.³¹ Suspended particles of different densities and fluorescent dye were used to visualize the flow. Once the tank was at the desired inclination angle, enough time was allowed for the fluid to settle to a state of practically no residual motion, and then the bottom heating was initiated. A CCD camera and a SVHS/VCR recorded the motion field in the tank. The particle paths so recorded were digitized and analyzed using the DigImage software package.³² The heat input during most of the critical-angle experiments was fixed at 1000 W/m^2 to ensure turbulent motion.

For the purpose of quantifying the observations, the critical slope angle (β_c) was defined as a limiting value of the slope inclination angle β below which upslope flow is

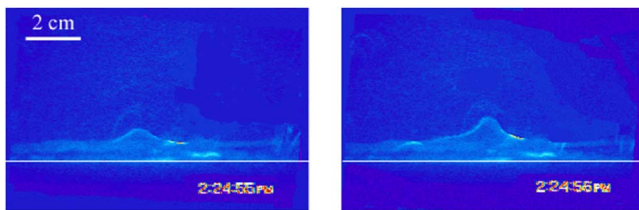


FIG. 6. (Color online) The formation of thermals on a heated horizontal plane ($Q=500 \text{ W/m}^2$).

not discernible, i.e., vertical rising of thermals dominates the flow. For each mixture of water and glycerin, an initial experiment was performed using a large slope angle where well-developed upslope motion existed. This experiment was then repeated, but with a 0.125° reduction of the slope angle, until mean upslope flow was no longer dominant over vertical rising of thermals. Several more experiments were conducted with subcritical and supercritical slopes to ensure the accuracy of β_c . Separate detailed flow visualization experiments were performed to delineate the mechanisms of blob growth. In these experiments homogeneous salt water of density 1.035 g/cm^3 was used and fluorescent dye was slowly injected onto the incline. In both types (aqueous glycerin and salt water) of experiments, particles in the flow were illuminated using a 2 mm thick light sheet entering through a slit from the top opening of the tank. Particle paths recorded were later evaluated to determine the velocity structure near the heated wall.

IV. EXPERIMENTAL RESULTS

Figure 6 shows the formation of a single thermal on a horizontal surface, as visualized by placing a thin sheet of fluorescent dye on the heating surface at the start of the experiment. Note the formation of thermal due to the breakdown of the near-wall thermal boundary layer, as discussed in Sec. II. Figure 7 shows a sloping counterpart of the above experiments. Careful observations show that the initial development of thermals is much the same as in Fig. 6, but with time the thermals grow asymmetrically. The corresponding velocity vectors are shown in Fig. 8, where the

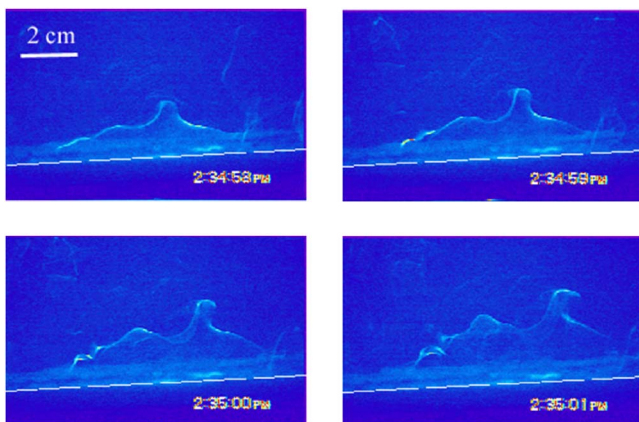


FIG. 7. (Color online) Thermal formation on an inclined surface ($\beta=3^\circ$, $Q=500 \text{ W/m}^2$). The picture was taken 1 min after initiation of heating.

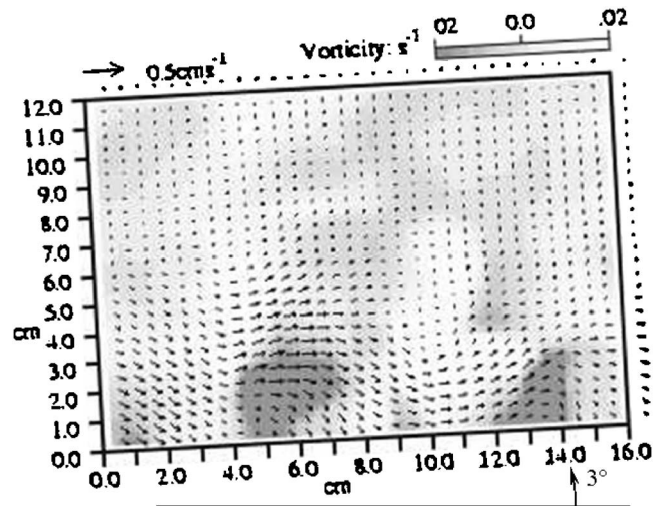


FIG. 8. Turbulent convection-instantaneous velocity and vorticity fields ($\beta=3^\circ$, $Q=300 \text{ W/m}^2$, $\text{Pr}=10$) taken 1 min after the initiation of heating.

velocity field associated with conventional thermals and the upslope flow are evident; these are the type of plots used for ascertaining the presence of upslope flow and hence in determining β_c .

The experiments showed that, from the very beginning of its formation, the blob is following the slope. This can be attributed to the sliding of the buoyancy induced blobs along the slope according to Eq. (2). The flow appears to be laminar. If the heat flux is strong enough to drive the turbulent flow, then the blob, while growing, is advected by this laminar upslope flow and then detaches from the heated surface after traveling a length given by Eq. (6). These detached and deflected blobs contribute to the maintenance of turbulent upslope flow. Figure 9 shows the initial development of the thin boundary layer that slides along the slope, the emergence of blobs from this layer and their detachment as rising thermals which carry heat (buoyancy) from the heated plate.

In experiments with very high Pr (>20 , even with a heat flux of 1000 W/m^2) or with very low heat flux, although an upslope flow is present, the vigorous thermal activity is essentially absent, as indicated in Fig. 10 for heat flux $Q=30 \text{ W/m}^2$ and Prandtl number $\text{Pr}=10$. Owing to the lack of distinct blob formation, the expression (14) is not expected to hold for this case. One may argue that the disappearance of blob formation is related to both the heat flux (intensity of turbulent flow) and Pr , but the effect of the former was not systematically investigated in the present study. A further discussion on this aspect is given in Sec. V.

A large number of experiments were conducted covering a substantial Prandtl number range, from 6 (pure water) to 9500 (pure glycerin), and for each case β_c was determined.

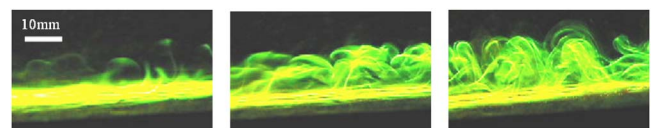


FIG. 9. (Color online) The formation of thermals on a sloping plane ($\beta=3^\circ$, $Q=1000 \text{ W/m}^2$). Pictures were taken 2 s apart.

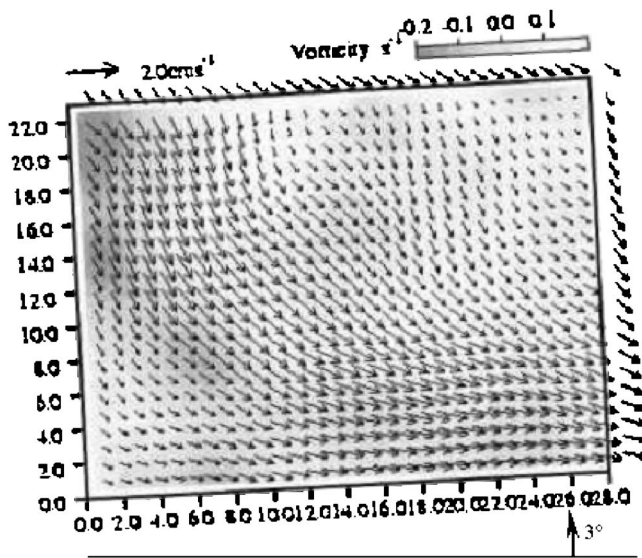


FIG. 10. Convection on a slope at low heat fluxes ($\beta=3^\circ$, $Q=30 \text{ W/m}^2$, $\text{Pr}=10$) taken after 1 min of heating.

An error analysis was also conducted by considering the uncertainties of temperature dependence of Pr and the measurements of heat flux and angle. The results of β_c as a function of Pr are shown in Fig. 11. Figure 11(a) shows results for $\text{Pr}<20$ and a heat flux range of $0.7\text{--}1 \text{ kW/m}^2$ (which ensured that blob formation and growth preceded the upslope flow). Note the proportionality between β_c and Pr with a proportionality constant of $c \approx 3 \times 10^{-3}$ for $\text{Pr}<20$. Figure

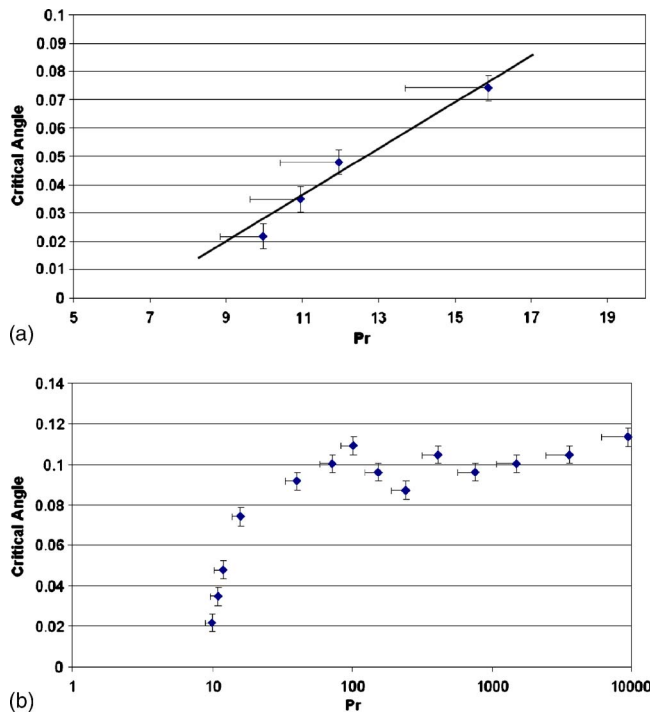


FIG. 11. (Color online) (a) Critical angle (β_c) dependence on the Prandtl number (Pr) for $\text{Pr}<20$. A linear fit is presented. Surface heat flux was 1000 W/m^2 . (b) Critical angle (β_c) dependence on the Prandtl number (Pr) for the entire range investigated with surface heat flux of 1000 W/m^2 . For $\text{Pr}>20$ a laminar upslope flow layer became evident without forming thermals during the initial development of the upslope flow.

11(b) presents the whole range of Prandtl numbers investigated for runs conducted with 1 kW/m^2 heat flux. At larger $\text{Pr}>20$, $\beta_c=c \text{ Pr}$ does not hold, whereas the flow was more streamlined without any observational evidence of thermal detachment (Fig. 10). In this case, the mechanism considered in Sec. II is not expected to be valid.

V. SUMMARY AND DISCUSSION

The aim of this study was to investigate the critical slope angle above which an upslope flow is initiated above a sloping, uniformly heated flat surface. Simple scaling arguments showed that the ratio of vertical to horizontal forcing on isolated thermals developing on the heated surface is proportional to the Prandtl number (Pr) and inversely proportional to the slope angle (β), and thus the critical slope β_c beyond which a turbulent upslope flow can be sustained is given by $\beta_c=c \text{ Pr}$, where $c \approx 3 \times 10^{-3}$ is an empirical constant. This prediction was verified using laboratory experiments, wherein a wide range of Prandtl numbers was achieved using different water-glycerin solutions. The slope angle β was systematically changed, the bottom heating was kept uniform, and the heat flux was maintained sufficiently high to achieve turbulent flow conditions. The initial flow development was visualized using dye and quantitatively measured using a DigImage (Ref. 32) particle tracking velocimetry (PTV) system.

Observations showed that upon the introduction of surface heating a thin, laminar-like, upslope layer is formed, followed by the formation and growth of thermal blobs. It was found that for the heat fluxes used ($\sim 1 \text{ kW/m}^2$) the thermal growth mechanism is active at the onset of upslope flow only when $\text{Pr}<20$. This observation is consistent with the fact that the model developed is valid only when the momentum and thermal boundary layer thicknesses are on the same order or $\text{Pr}^{1/2} \sim 1$. At larger Prandtl numbers, the momentum boundary-layer thickness is larger than the thermal layer, and the velocity shear above the thermal layer can modify the thermal blob formation mechanism. Note that turbulent convection driven by thermal blobs occurs³³ only when the flux Rayleigh number, $\text{Ra}_f = q_0 H^4 / \kappa^2 \nu$, where H is the depth of the fluid layer, exceeds a critical value ($\sim 10^8$), and this criterion is satisfied in our laboratory experiments. Typical heat fluxes for the atmosphere are in the range of $300\text{--}600 \text{ W/m}^2$, and thus $\text{Ra}_f \sim 10^{19}$ and $\text{Pr} \sim 0.7$, which are also in parameter ranges conducive for thermal blob formation.

The present theoretical analysis as well as laboratory experiments considered an idealized case of uniform slope heating, smooth and flat surface, neutral initial stability, and no pre-existing flow prior to heating. In real atmospheric cases, however, the slope is rough, uneven, and nonuniformly heated; in the morning hours the air layer near the ground is stable, and pre-existing motions are the rule rather than the exception. Such effects can have a profound effect on the criterion for the initiation of anabatic flow, and hence extrapolation of present results to the atmosphere should be

done with caution. For example, stable stratification blocks the vertical rise of thermals and facilitates along-slope flow, nonuniformity of surface temperature causes local secondary flows on the incline,¹⁸ and pre-existing air motions can affect the mechanism of upslope flow generation.³⁴ Nonetheless, as discussed, the initiation of atmospheric upslope flow is expected to be associated with the thermal blob formation (given that $Pr^{1/2} \sim 1$) and thus the present work offers a framework to study more complicated cases of upslope flows found in nature. It should also be mentioned that the flow in water tank experiments utilized in our work has some dynamical equivalence to atmospheric convection, thus allowing extrapolation of results from one case to another.^{33,35}

Based on the idealized case addressed here, the critical angle β_c for the atmosphere ($Pr \sim 0.7$) is small, approximately 0.1° . This observation is consistent with numerous observations made in the atmosphere that even on gently sloping surfaces (e.g., as low as 0.18° in the Phoenix valley^{4,7}) a dominant upslope flow is present.⁷

ACKNOWLEDGMENTS

This research was supported by the U.S. National Science Foundation (ATM) and the Science Foundation of Arizona. The authors wish to acknowledge Mr. Gerardo Brigido for his help with laboratory experiments as a REU student. Two anonymous reviewers made valuable comments that considerably improved the quality of this paper.

- ¹C. D. Whiteman, *Mountain Meteorology: Fundamentals and Applications*, 1st ed. (Oxford University Press, Oxford, 2000), p. 355.
- ²C. D. Whiteman, "Observations of thermally developed wind systems in mountainous terrain," Chap. 2 in *Atmospheric Processes Over Complex Terrain*, Meteorological Monographs, edited by W. Blumen (American Meteorological Society, Boston, 1990), Vol. 23, p. 5.
- ³P. G. Baines, "Mixing in flows down gentle slopes into stratified environments," *J. Fluid Mech.* **471**, 315 (2002).
- ⁴A. W. Ellis, M. L. Hildebrandt, W. M. Thomas, and H. J. S. Fernando, "Analysis of the climatic mechanisms contributing to the summertime transport of lower atmospheric ozone across metropolitan Phoenix, Arizona, USA," *Clim. Res.* **15**, 13 (2000).
- ⁵H. J. S. Fernando, S. M. Lee, J. Anderson, M. Princevac, E. Pardyjak, and S. Grossman-Clarke, "Urban fluid mechanics: Air circulation and contaminant dispersion in cities," *Env. Fluid Mech.* **1**, 107 (2001).
- ⁶S. M. Lee, H. J. S. Fernando, and S. Grossman-Clarke, "MM5-SMOKE-CMAQ as a modeling tool for 8-h ozone regulatory enforcement: Application to the state of Arizona," *Environ. Model. Assess.* **12**, 63 (2007).
- ⁷J. C. R. Hunt, H. J. S. Fernando, and M. Princevac, "Unsteady thermally driven flows on gentle slopes," *J. Atmos. Sci.* **60**, 2169 (2003).
- ⁸H. D. Orville, "On mountain upslope winds," *J. Atmos. Sci.* **21**, 622 (1964).
- ⁹R. M. Banta, "Daytime boundary layer evolution over mountainous terrain. Part I: Observations of the dry circulations," *Mon. Weather Rev.* **112**, 340 (1984).
- ¹⁰R. M. Banta, "Daytime boundary layer evolution over mountainous ter-

- rain. Part II: Numerical studies of upslope flow duration," *Mon. Weather Rev.* **114**, 1112 (1986).
- ¹¹J. Kondo, T. Kuwagata, and S. Haginoya, "Heat budget analysis of nocturnal cooling and daytime heating in a basin," *J. Atmos. Sci.* **46**, 2917 (1989).
- ¹²T. Kuwagata and F. Kimura, "Daytime boundary layer evolution in a deep valley. Part II: Numerical simulation of the cross valley circulation," *Bull. Am. Meteorol. Soc.* **36**, 883 (1997).
- ¹³B. W. Atkinson and A. N. Shahub, "Orographic and stability effects on daytime, valley-side slope flows," *Boundary-Layer Meteorol.* **68**, 275 (1994).
- ¹⁴L. Prandtl, *Essentials of Fluid Dynamics* (Hafner, New York, 1952), p. 452.
- ¹⁵J. Egger, "On the linear two-dimensional theory of thermally induced slope winds," *Beitr. Phys. Atmos.* **54**, 465 (1981).
- ¹⁶U. Schumann, "A simple model of the convective boundary layer over wavy terrain with variable heat flux," *Beitr. Phys. Atmos.* **64**, 169 (1991).
- ¹⁷U. Schumann, "Large-eddy simulation of the up-slope boundary layer," *Q. J. R. Meteorol. Soc.* **116**, 637 (1989).
- ¹⁸I. Vergeiner and E. Dreiseitl, "Valley winds and slope winds—observations and elementary thoughts," *Meteorol. Atmos. Phys.* **36**, 264 (1987).
- ¹⁹J. W. Deardorff and G. E. Willis, "Turbulence within a baroclinic laboratory mixed layer above a sloping surface," *J. Atmos. Sci.* **44**, 722 (1987).
- ²⁰J. A. King and D. D. Ribble, "Laminar natural convection heat transfer from inclined surfaces," *Int. J. Heat Mass Transfer* **34**, 1901 (1991).
- ²¹J. A. King, "Natural convections above heated surfaces," Ph.D. thesis, Chemical Engineering Department, Louisiana State University (1990).
- ²²G. Rampanelli, D. Zardi, and R. Rotunno, "Mechanisms of up-valley winds," *J. Atmos. Sci.* **61**, 3097 (2004).
- ²³B. W. Atkinson, *Mesoscale Atmospheric Circulations* (Academic, London, 1981), p. 279.
- ²⁴J. C. R. Hunt, "Industrial and environmental fluid mechanics," *Annu. Rev. Fluid Mech.* **23**, 1 (1991).
- ²⁵L. N. Howard, "Convection at high Rayleigh number," in *Applied Mechanics, Proceeding of the 11th Congress of Applied Mechanics*, edited by H. Görtler (Springer, Munich, 1966), p. 1109.
- ²⁶E. M. Sparrow, R. B. Husar, and R. J. Goldstein, "Observations and other characteristics of thermal," *J. Fluid Mech.* **41**, 793 (1970).
- ²⁷R. J. Adrian, R. T. D. S. Ferreira, and T. Boberg, "Turbulent thermal convection in wide horizontal fluid layers," *Exp. Fluids* **4**, 121 (1986).
- ²⁸I. Reba, "Applications of the Coanda effect," *Sci. Am.* **214**, 84 (1966).
- ²⁹J. S. Turner, *Buoyancy Effects in Fluids* (Cambridge University Press, Cambridge, 1979), p. 367.
- ³⁰S. I. Voropayev and H. J. S. Fernando, "Evolution of two-layer thermohaline systems under surface cooling," *J. Fluid Mech.* **380**, 117 (1999).
- ³¹P. N. Shankar and M. Kumar, "Experimental determination of the kinematic viscosity of glycerol-water mixtures," *Proc. R. Soc. London, Ser. A* **444**, 573 (1994).
- ³²S. B. Dalziel, "Rayleigh-Taylor Instability: experiments with image analysis," *Dyn. Atmos. Oceans* **20**, 127 (1993).
- ³³J. W. Deardorff and G. E. Willis, "Further results from a laboratory model of the convective planetary boundary layer," *Boundary-Layer Meteorol.* **32**, 205 (1985).
- ³⁴M. H. Dickerson and P. H. Gudiksen, "Atmospheric studies in complex terrain," Technical Progress Reports FY-1979–FY-1983, No. ASCOT 84-1/UCID-19851, U.S. Department of Energy, Lawrence Livermore National Laboratory, Livermore, CA (1984).
- ³⁵R. R. Chen, N. S. Berman, D. L. Boyer, and H. J. S. Fernando, "Physical model of diurnal heating in the vicinity of a two-dimensional ridge," *J. Atmos. Sci.* **53**, 62 (1996).